



25<sup>th</sup> ABCM International Congress of Mechanical Engineering  
October 20-25, 2019, Uberlândia, MG, Brazil

**COB-2019-1071**

## **KINEMATIC CALIBRATION OF A 6-D.O.F. MANIPULATOR USING A MODEL OPTIMIZATION ROUTINE**

**Patrícia da Silva Oliveira**

**José Maurício Santos Torres Motta**

Universidade de Brasília, Departamento de Engenharia Mecânica, Campus Darcy Ribeiro, Brasília-DF, 70.910-900, Brasil

patricia.silva.oliver@gmail.com; jmmotta@unb.br

**Abstract.** *The use of robots in different manufacturing processes, as well as the use of offline programming in the manipulators, aiming to maximize their working time, have gradually increased. However, the success of offline programming is directly related to the good repeatability and accuracy of the robot, and the values of the latter factor are usually worse than the first. A viable and inexpensive way that can improve the accuracy of manipulators is the robot calibration, which can be statically or dynamically. Since geometric errors correspond to about 90% of all robot errors, the static calibration process is the most used. Thus, this article aims to investigate some theoretical aspects of robot calibration using parametric error modeling, performing a computational simulation of the calibration process of an ABB IRB-140 six degrees of freedom manipulator. For this, kinematic modeling was first carried out, followed by the identification and optimization of the model. Among the results obtained, an optimized model with 24 parameters was obtained, free of deficiencies and redundancies. In addition, it was also observed that a set with more than 40 points provides an irrelevant improvement in calibration accuracy.*

**Keywords:** *robot calibration, model parameter optimization, accuracy improvement, parameter redundancies, numerical improvement*

### **1. INTRODUCTION**

According to Ginani and Motta (2011), for a long time robots were employed in manufacturing processes, with the aim of replacing human labor in unhealthy and repetitive tasks. However, with the diversification and expansion of robotic applications, there was a need to improve the accuracy of trajectories obtained through off-line programming (Yang *et al.*, 2014), which consists of the technique of programming the robot without using the actual machine in fact (Motta, 2006). In the industry shop-floor, the importance of off-line programming has been growing steadily, due to the urgency of decreasing the downtime of the machine, and consequently increasing the working time of the robot (Motta, 2006). In order to illustrate the importance of this type of programming, according to Motta and McMaster (1999), a welding line with 30 robots and 40 welding points per robot it takes, approximately, 400 hours to program them.

However, despite the advantages of off-line programming over online programming, its success depends directly on the good repeatability and accuracy of the robot (Motta, 2006). Gao *et al.* (2018) add that, in industrial robotic applications, positioning accuracy is a critical factor, especially in the areas of welding, assembly, etc. According to (Ha, 2008), robots in general have high repeatability over their accuracy, which implies that the problem is to improve and maintain the accuracy of the system in various manufacturing environments. In numerical terms, the repeatability of the manipulators' position is better than 1 mm, whereas the accuracy with which the robot can reach a certain position and orientation in relation to an external or working coordinate system, has worse values (Duelen and Schröder, 1991).

In this context, a robotic manipulator is subject to numerous sources of positioning errors. A priori, these errors can be grouped into two large groups: geometric errors, which result from the imprecision of the manufacturing processes and joint errors, and non-geometric errors, arising from the action of the gravity and inertial forces causing joint deformation, as well as numerical errors (Jang *et al.*, 2001). According to Duelen and Schröder (1991), the position errors are caused by differences between the actual and nominal dimensions of the robot, and due to elastic and plastic deformations of the material. These errors are systematic and deterministic, and can be compensated, once the parameters of each robot are known.

In view of this, it is evident the need of methods to improve the accuracy of the manipulators. Among the existing methods, robot calibration is easy to implement and its cost is relatively low (Liu *et al.*, 2016). From a mathematical point of view, robot calibration is defined as the sequence of non-linear parameter estimates, whose unknown errors are identified by minimizing a cost function (Motta *et al.*, 2016), and make the mathematical model closer to the experimental data considered. In general, calibration is divided into two categories: kinematic calibration (compensation of geometric

errors) and dynamic calibration (compensation of non-geometric errors) (Liu *et al.*, 2016). According to Motta (2005), the geometric errors correspond to about 90% of all the errors of the robot, which justifies the fact that the kinematic calibration process, also called static calibration, is widely used. In general, manipulators have positioning errors between 5 and 15 mm (even if they are new), and, after being properly calibrated, these errors can be reduced to values smaller than 0.5 mm.

According to Motta (2005), the robot calibration comprises four steps: modeling, measurement, numerical identification of the real physical characteristics of the robot and implementation of a new model or coordinate compensation. According to Motta (1999), kinematic modeling consists of obtaining a mathematical model representative of the geometry and movement of the robot; during the measurement step, however, specific geometric characteristics of the robot are measured with the aid of measuring equipment with known accuracy; in the third step (identification), on the other hand, the values of the parameters of the model are identified; Finally, the model is corrected in the control system of the robot, aiming to succeed in performing scheduled tasks.

Therefore, this research aims to investigate theoretical aspects of robot calibration, performing a computational simulation of the calibration process in a six degree-of- freedom manipulator (D.O.F.). The main contribution of this article is a mathematical procedure to detect redundant and unidentifiable error parameters in the manipulator kinematic model, since the precision and reliability of the identified error parameter values depend on the number of the error parameters included in the model Bernard and Albright (1993). The use of this optimization technique improves the condition number of the system, reduces the number of measurement points required and improves the robot positioning accuracy. This work is organized as follows: Section 2 shows the kinematic modeling for the IRB-140 manipulator from the conventions of Denavit and Hartenberg and Hayati and Mirmirani; in Section 3 the parameterization of the kinematic model is developed to identify the parameters; Section 4 presents pertinent fundamentals for model optimization; in Section 5, the results obtained in the calibration evaluation are discussed; and, in Section 6, the conclusions of the work are shown.

## 2. KINEMATIC MODELING

According to Bernard and Albright (1993), the calibration process is based on a mathematical model of the physical robot, which includes all significant and deterministic sources of position errors. For calibration purposes, the robot is considered as a static system described by a model function, whose input values are joint angles, and the output values are the position and orientation of the coordinate system located at the center point of the tool (TCP). This function is called by Santolaria *et al.* (2008) as a direct kinematic model, and assumes the form expressed by Eq. (1).

$$y = f(\theta_i, q) \quad (1)$$

In Equation (1),  $i = 1, \dots, n$  corresponds to the number of rotating joints. This model calculates the position and the orientation  $y$  of TCP, according to the value of the joint variables  $\theta_i$  and the equations of the model defined in  $f$ , which depend on parameters of the vector  $q$  to be optimized to obtain the smallest possible measurement error.

According to Motta (1999) and Motta *et al.* (2001), the first stage of kinematic modeling implies the assignment of an orthogonal coordinate system for each robot link. Thus, initially the  $z$  should be made to coincide with the joint axis so that if the joint is prismatic the direction of the  $z$  corresponds to the direction of motion and its direction is along the joint; if the joint is of revolution, however, the direction of the  $z$  is in the positive direction of rotation about the  $z$ . The base coordinate system can be defined with axes parallel to the world coordinate system. The origin of the base coordinate system is coincident with the origin of the joint 1 (first joint), which assumes that the joint axis 1 is normal to the  $x$ - $y$  plane. Then the coordinate systems are inserted into the loop at your distal joint. A system is internal to the link to which it is connected, and the next link moves in relation to it, ie the coordinate system  $i$  is in the  $i+1$  junction. In relation to the origin of the other coordinate systems, if the axes of a link intercept, the origin of the system connected to the link is inserted at the intersection of the joint axes, on the other hand, if the axes of the joints are parallel, then the origin of the joint is placed in the distal joint. Subsequently, if the origin of a system is described in relation to another coordinate system using more than one direction, then it must be moved to use only one direction.

Therefore, the origins are described using the least number of link parameters. The axes  $x$  and  $y$  have their direction defined according to the convention used to parameterize the transformations between the links, and can be obtained from the rule of the right hand. The TCP coordinate system has the  $z$  axis in the same direction as the  $z$  axis of the last nested joint  $n-1$  coordinate system. From this convention, geometric parameters of length are established:  $p_{ni}$  (distance between the coordinate systems  $i-1$  and  $i$ ), and  $n$  is the parallel axis located in the  $i-1$  coordinate system.

Applying the right rules to the IRB-140 manipulator, the coordinate systems for each robot joint is obtained, as shown in Fig. 1.

The homogeneous transformations used in the kinematic modeling were constructed in order to ensure that the model is complete, continuous and minimal, which means that the Denavit-Hartenberg (DH) convention was used for perpendicular rotary joints, while the Hayati-Mirmirani (HM) convention was used for parallel rotary joints, avoiding singularities

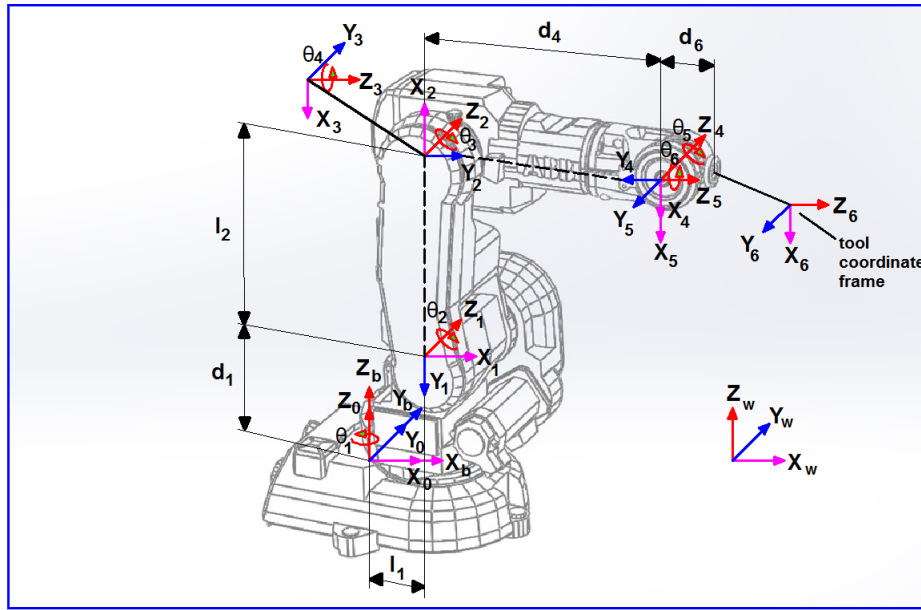


Figure 1. Coordinate systems and geometrical parameters of the IRB-140.

in the error model Jacobian (Schröder *et al.*, 1997) and (Motta, 1999). The elementary transformations for IRB-140 are grouped in Tab. 1.

Table 1. Elementary transformation for the IRB-140.

Transformation	Joint Type	Parametrization
World frame to base frame	W-B	$[T_x(pxb).T_y(pyb).T_z(pzb).R_x(\delta xb).R_y(\delta yb).R_z(\delta zb)]$
Joint 0 to Joint 1	$J_R \perp J_R$	$[R_z(\theta_1).T_z(pz_1).T_x(px_1).R_x(\alpha_1)]$
Joint 1 to Joint 2	$J_R \perp J_R$	$[R_z(\theta_2).T_z(pz_2).T_x(px_2).R_x(\alpha_2)]$
Joint 2 to Joint 3	$J_R \parallel J_R$	$[R_z(\theta_3).T_x(px_3).R_x(\alpha_3).R_y(\beta_3)]$
Joint 3 to Joint 4	$J_R \perp J_R$	$[R_z(\theta_4).T_z(pz_4).T_x(px_4).R_x(\alpha_4)]$
Joint 4 to Joint 5	$J_R \perp J_R$	$[R_z(\theta_5).T_z(pz_5).T_x(px_5).R_x(\alpha_5)]$
Joint 5 to Joint 6	$J_R \parallel TCP$	$[R_z(\theta_6).T_x(px_6).T_y(py_6).T_z(pz_6)]$

$W = world, B = base, R = rotary, \perp = perpendicular$

### 3. PARAMETER IDENTIFICATION

The kinematic equations of the manipulator are determined from the product between the homogeneous transformations of the base coordinate system and the TCP coordinate system, as expressed by Eq. (2).

$$\hat{T}_N^0 = \hat{T}_N^0(k) = T_1^0.T_2^1 \dots T_N^{N-1} = \prod_{i=1}^N T_i^{i-1} \quad (2)$$

In Equation (2),  $N$  corresponds to the number of joints. The vector containing the parameters with their respective errors ( $p = [p_1^T p_2^T \dots p_n^T]^T$ ) may be included in the transformations, so that the exact transformation of the manipulator is now indicated by Eq. (3).

$$A_i^{i-1} = T_i^{i-1} + \Delta T_i; \Delta_i = \Delta T_i(\Delta p_i) \quad (3)$$

where  $\Delta p_i$  is the vector of loop parameter errors for the joint  $i$ . Therefore, the transformation of the last coordinate system to the first coordinate system (with the errors of the parameters) is given by Eq. (4).

$$\hat{A}_N^0 = \hat{T}_N^0 + \Delta \hat{T}, \Delta \hat{T} = \Delta \hat{T}(q, \Delta p) \quad (4)$$

In Equation (4),  $\Delta\hat{T}$  is a nonlinear function,  $\Delta p = [\Delta p_1^T \Delta p_2^T \dots \Delta p_n^T]^T$  is the vector of error parameters of the manipulator, and  $q$  is the vector of joint variables  $[\theta_1^T, \theta_2^T, \theta_N^T]^T$ . For  $m$  measured positions, we have the Eq. (5) and Eq. (6), in which  $n$  is the number of parameters and  $n$  is the number of joints (including tool).

$$\hat{\mathbf{A}} = \hat{\mathbf{A}}_N^0 = \hat{\mathbf{A}}(\mathbf{q}, p) = (\hat{A}(q_1, p), \dots, \hat{A}(q_m, p))^T : \mathbb{R}^n \times \mathbb{R}^{mn} \quad (5)$$

$$\Delta\hat{\mathbf{T}} = \Delta\hat{\mathbf{T}}(\mathbf{q}, \Delta p) = (\Delta\hat{T}(q_1, \Delta p), \dots, \Delta\hat{T}(q_m, \Delta p))^T : \mathbb{R}^n \times \mathbb{R}^{mn} \quad (6)$$

The identification process consists in making an ideal adjustment between the real positions (obtained by means of measuring instruments) and the positions calculated by the kinematic model, resulting in the solution of a system of non-linear equations represented by Eq. (7).

$$\mathbf{B}(\mathbf{q}, q^*) = \mathbf{M}(\mathbf{q}) = \mathbf{B}(\mathbf{q}, p) + \mathbf{C}(\mathbf{q}, \Delta p), \epsilon \mathbb{R}^{\phi m} \quad (7)$$

In Equation (7),  $\phi$  is the number of equations arising from each measurement position,  $\mathbf{B}$  is a vector formed by the position and orientation components of  $\hat{\mathbf{A}}$ ,  $\mathbf{M}$  corresponds to the measured components and  $\mathbf{C}$  is the vector of differential motion formed by the rotation and position components of  $\Delta\hat{\mathbf{T}}$ . If only position data are considered (as is the case of the present work), each position measurement will provide three equations, and  $\mathbf{B}$  will only include position components. Because this is a problem where you are trying to fit data into a nonlinear model, nonlinear least squares is the most recommended numerical method of solution (Motta *et al.*, 2001). Neglecting the second-order products of the Jacobian matrix, we have the mathematical expression for  $\mathbf{C}$  in Eq. (8).

$$\mathbf{C}(\mathbf{q}, \Delta p) = \mathbf{J} \cdot \Delta p \quad (8)$$

By replacing the equation (8) in Eq. (7) and rearranging the terms, we obtain the mathematical model represented by Eq. (9).

$$\mathbf{M}(\mathbf{q}) - \mathbf{B}(\mathbf{q}, q) = \mathbf{J} \cdot \Delta p \quad (9)$$

The notation present in Eq. (10), Eq. (11) and Eq. (12) allow to rewrite Eq. (9) to Eq. (13).

$$\mathbf{b} = \mathbf{M}(\mathbf{q}) - \mathbf{B}(\mathbf{q}, p), \epsilon \mathbb{R}^{\phi m} \quad (10)$$

$$\mathbf{J} = \mathbf{J}(\mathbf{q}, \Delta p), \epsilon \mathbb{R}^{\phi m \times n} \quad (11)$$

$$x = \Delta p, \epsilon \mathbb{R}^n \quad (12)$$

$$\mathbf{r} = \mathbf{J} \cdot x - \mathbf{b}, \epsilon \mathbb{R}^{\phi m} \quad (13)$$

Equation (13) can be solved by the non-linear least squares method in the form of Eq. (14).

$$\mathbf{J} \cdot x = \mathbf{b} \quad (14)$$

The least squares problem can be solved by the method proposed by Levenberg-Marquardt. Based on Eq. (9) and Eq. (14), this method can be formulated by Eq. (15).

$$x_{j+1} = x_j - [\mathbf{J}(x_j)^T \cdot \mathbf{J}(x_j) + \mu_j \cdot \mathbf{I}]^{-1} \cdot \mathbf{J}(x_j) \cdot \mathbf{b}(x_j) \quad (15)$$

In Equation (15),  $\mu_j$  is obtained by means of the relations shown in Eq. (16).

$$\left\{ \begin{array}{l} \mu_j = 0.001 \\ \mu_j = \lambda \cdot 0.001 \rightarrow \text{if } |\mathbf{b}(x_{j+1})| \geq |\mathbf{b}(x_j)| \\ \mu_j = \frac{0.001}{\lambda} \rightarrow \text{if } |\mathbf{b}(x_{j+1})| \leq |\mathbf{b}(x_j)| \\ \mu_j = 2.5 < \lambda < 10 \end{array} \right. \quad (16)$$

The parameterized error kinematic models for robot calibration must have three important properties: completeness, continuity and minimality (Schröer *et al.*, 1997) and (Motta *et al.*, 2016). Table 2 shows the IRB-140 transformations with the added error parameters.

Table 2. Parametric transformations for the IRB-140.

Joint Type	D-H Parametrization
W-B	$[T_x(px_b + \delta px_b).T_y(py_b + \delta py_b).T_z(pz_b + \delta pz_b).R_x(\alpha_b + \delta \alpha_b).R_y(\beta_b + \delta \beta_b).R_z(\gamma_b + \delta \gamma_b)]$
$J_R \perp J_R$	$[R_z(\theta_1 + \delta \theta_1).T_z(pz_1 + \delta pz_1).T_x(px_1 + \delta px_1).R_x(\alpha_1 + \delta \alpha_1)]$
$J_R \perp J_R$	$[R_z(\theta_2 + \delta \theta_2).T_z(pz_2 + \delta pz_2).T_x(px_1 + \delta px_1).R_x(\alpha_1 + \delta \alpha_1)]$
$J_R \parallel J_R$	$[R_z(\theta_3 + \delta \theta_3).T_x(px_3 + \delta px_3).R_x(\alpha_3 + \delta \alpha_3).R_y(\beta_3 + \delta \beta_3)]$
$J_R \perp J_R$	$[R_z(\theta_4 + \delta \theta_4).T_z(pz_4 + \delta pz_4).T_x(px_4 + \delta px_4).R_x(\alpha_4 + \delta \alpha_4)]$
$J_R \perp J_R$	$[R_z(\theta_5 + \delta \theta_5).T_z(pz_5 + \delta pz_5).T_x(px_5 + \delta px_5).R_x(\alpha_5 + \delta \alpha_5)]$
$J_R \parallel TCP$	$[R_z(\theta_6 + \delta \theta_6).T_x(px_6 + \delta px_6).T_y(py_6 + \delta py_6).T_z(pz_6 + \delta pz_6)]$

It can be observed in Table 2 that the maximum number of parameters to be identified is 30.

#### 4. MODEL OPTIMIZATION

The optimization of the kinematic model implemented in this work, aiming to improve the step of identifying the parameters through the elimination of dependencies or redundancies, includes the decomposition into singular values, the Jacobian column staggering and the Jacobian matrix conditioning number analysis.

The Decomposition in Singular Values (SVD), used by Wampler *et al.* (1990), Motta (1999), Bai and Teo (2003) and Agheli and Nategh (2009), consists of a numerical technique used in linear algebra of ill-conditioned problems. In addition, SVD allows you to adequately handle overdetermined problems and provides a diagnosis of where the difficulty is in solving the problem. The Jacobian matrix used in the identification of the parameters is indicated in Eq. (17).

$$J_{3m \times p} = U_{3m \times 3m} \cdot S_{3m \times p} \cdot V_{p \times p}^T \quad (17)$$

In Equation (17),  $U$  e  $V$  are unitary orthogonal arrays and  $S$  is a diagonal matrix whose elements of the main diagonal are singular values, which can be organized in descending order.

In problems involving matrices, the number of conditioning is important because it acts as a factor of amplification of error and perturbation analysis (Bernard and Albright, 1993). The conditioning number is defined by Eq. (18).

$$k(J) = \|J\| \cdot \|J^+\| \quad (18)$$

in which  $J^+$  corresponds to the pseudo-inverse of  $J$ . If the matrix norm is derived from the Euclidean vector norm, the number of conditioning is determined by Eq. (19), which relates the largest ( $S_1$ ) and the lowest ( $S_r$ ) singular values other than zero.

$$k(J) = \frac{S_1}{S_r} \quad (19)$$

According to Bernard and Albright (1993) and Motta (1999), the Jacobian column staggering is added to the identification optimization procedure in order to improve the conditioning of the problem. Models based on factor scaling can be estimated from robot errors (approximately 1 mm). Taking this into account, one can use Eq. (20) to obtain the stepped singular values.

$$\sigma p_i(q) = \frac{10^{-3}}{\left\| \frac{\partial}{\partial p_i} T(p, q) \right\|} \quad (20)$$

In equation (20)  $\sigma p_i(q)$  is the singular value of the parameter  $p_i$  in position  $q$ . Therefore, the routine implemented in this work to optimize the parametrized kinematic model, aiming to improve the parameter identification through the elimination of dependencies or redundancies, uses the Singular Value Decomposition (SVD), a Jacobian column scaling and analysis of the Jacobian matrix conditioning number. The optimization procedure has two steps:

1. Scaling the Jacobian matrix error parameters of the identification model, aiming to reduce the Jacobian condition number  $k(J)$ ;
2. If  $k(J)$  is above 100, a second step is followed to identify which model parameter is producing the solution of the error parameters to be deficient. This is performed by searching the smaller singular value  $S_r$  in the last column of matrix  $V$ .

This implies that an optimized model is obtained from the complete model by excluding a small number of parameters until  $k(J)$  is below 100.

## 5. RESULTS AND DISCUSSION

The computer simulation of the robot calibration process comprises all steps of a real calibration, i.e., kinematic modeling, parameter identification using some selected positions (measurements) and the accuracy evaluation. In this article, the simulations were performed using the IRB-140 manipulator, which has six degrees-of-freedom. Two kinematic models were used: *Simulated Pose Model* and *Estimated Pose Model*. The first model includes the geometric parameters and the addition of random errors in the variables of joints, allowing to simulate measurements of the TCP positions; the second model, on the other hand, contains all sources of geometric errors identified in the first model, except for the errors of the parameters that were eliminated in order to improve the identifiability of the model.

In this simulation, only position data were used, due to the types of measurement systems normally used. In mathematical terms, each measurement point provided three measurement equations. In order to minimize measurement noise, the number of equations must be two to three times larger than the number of parameters to be estimated. For the IRB-140, the maximum number of parameters is 30, which resulted in the choice of 30 measurement points (Zhuang and Roth, 1996). The set of deviations to be added to the values of the kinematic parameters of the robot was selected randomly between  $\pm 1$  mm for the translation parameters and  $\pm 0.0005$  rad for the orientation parameters. Concerning the measurement system, this was simulated from the addition of random errors, uniformly distributed between 0 and 1, to the exact homogeneous transformations of the robot model.

The first step of the robot calibration process uses the parameter model optimization routine, consisting in selecting the identifiable parameters from the analysis of the conditioning number of the Jacobian matrix by using the SVD. Figure 2 shows the evolution of the condition number as a function of the number of model parameters.

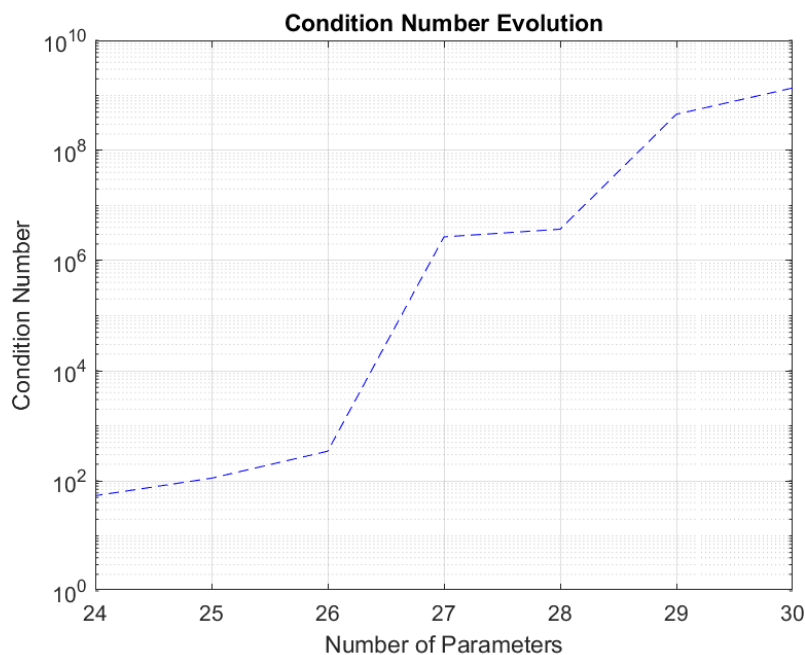


Figure 2. Calculated Condition Number of the Jacobian matrix during the identification step as a function of the number of parameters.

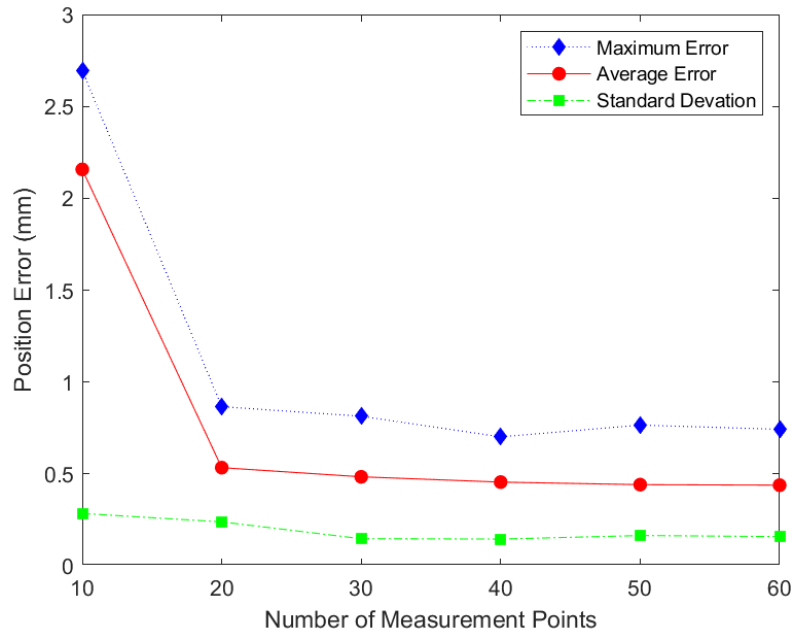


Figure 3. Robot accuracy as a function of the number of measurement points.

A brief analysis of Fig. 2 makes it possible to verify that, for 30 parameters, the condition number is of the order of  $10^9$ . This indicates a poorly conditioned solution, which can lead to a larger number of iterations for the convergence by the Levenberg-Marquardt algorithm, or the possibility of a local minimum being achieved even with a good convergence, or both. In addition, it is observed that, as the number of parameters decreases (through analysis of the last column of matrix  $V$ , indicating which parameters cause deficiencies or redundancies in the model), the condition number also decreases. Thus, a model with 24 parameters was reached, whose condition number equals 54.

In addition, with the minimum number of error parameters in the model, the influence of the number of measurement points on the robot accuracy was evaluated considering data sets with 10, 20, 30, 40, 50 and 60 points. The Figure 3 shows the curves for the mean and maximum position errors, with their respective standard deviations, from which it is possible to ascertain that the robot accuracy is proportional to the number of measured points. However, there is an irrelevant improvement in the robot accuracy for sets above 40 points, demonstrating that a set with 30 points is enough perform the robot calibration process.

The Figure 4 shows the deviation in TCP for each point in the set of 30 measurements, using the minimum calibrated model with addition of random errors to simulate the measurement system. The investigation of the curve of Fig. 4 shows that the maximum position error is 0.74 mm, less than the accuracy required in the automotive industry (about 2.5 mm) in parts manufactured by robots programmed offline (Bernard and Albright, 1993).

The accuracy of the calibrated minimum model was also analyzed, and the results can be visualized in Fig. 5, where the mean error and standard deviation at each iteration were calculated, respectively, by Eq. (21) and (22).

$$\bar{E} = \frac{\sum_{i=1}^n |M_i - A_i|}{n} \quad (21)$$

$$\sigma = \sqrt{\frac{\sum_{i=1}^n (|M_i - A_i| - \bar{E})^2}{n}} \quad (22)$$

In the Equations (21) and (22),  $M$  are the robot positions measured,  $A$  are the calculated positions and  $n$  is the number of points measured. The results present in Fig. 5 express the effector positioning accuracy, calculated as the mean of the absolute values of the residual errors between the simulated position and the expected (nominal) position of the effector, at each iteration of the calibrated minimum model. In addition, the maximum error and the standard deviation are also indicated. Analyzing the graph, it is verified that the position errors were reduced from approximately 1.0 mm in the first iteration to 0.4 mm in the last iteration.

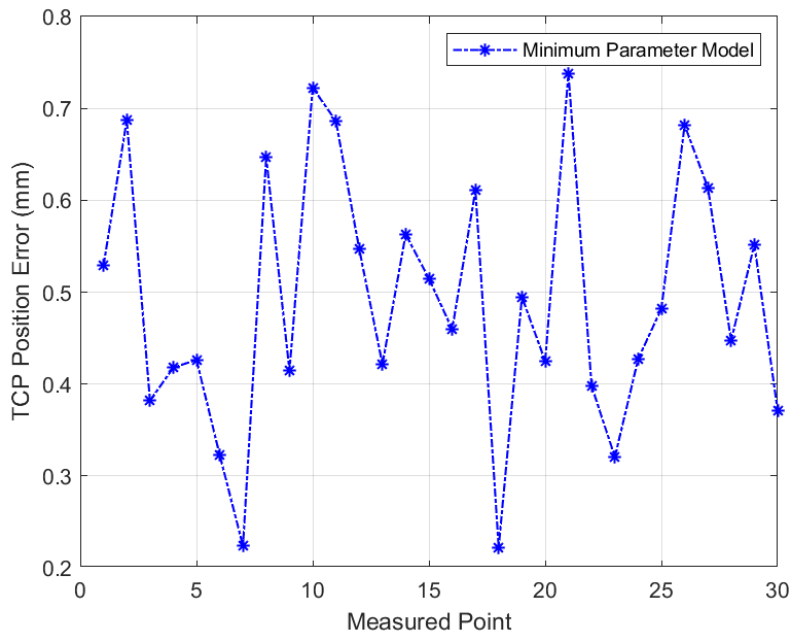


Figure 4. Positioning accuracy obtained by applying the optimized calibration model.

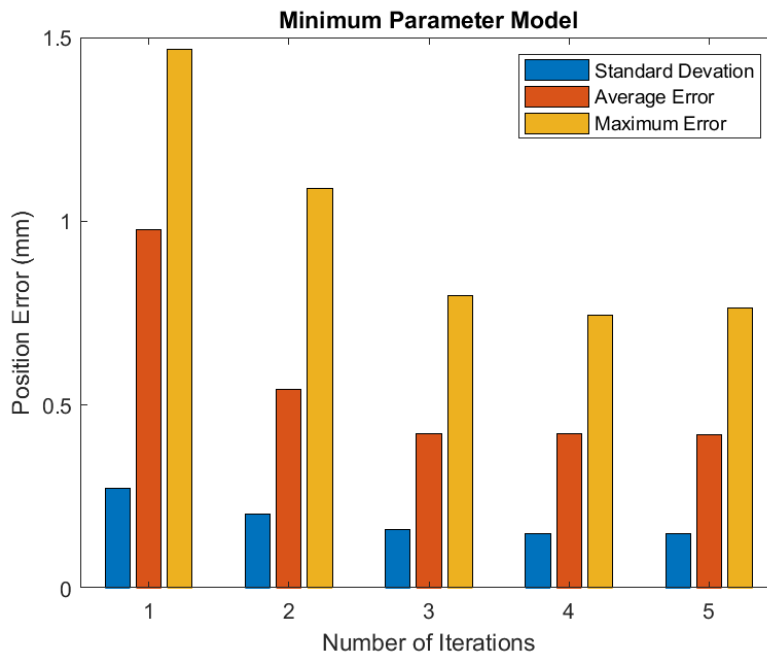


Figure 5. Evaluation of the calibrated model at each iteration.

## 6. CONCLUSION

In this work, a robot calibration methodology was presented using an optimization procedure to construct the error parameter model, aiming to eliminate deficiencies and redundancies of the parameters. To do so, a computational simulation was performed encompassing all steps of the calibration process. As results, it was verified that the Jacobian condition number of the model parameter matrix decreased as deficient and redundant parameters were eliminated, indicating an improvement in the process to identify kinematic model parameters that could be used to fit a model closer to the real robot. Furthermore, the influence of the number of measurement points on the robot accuracy after the calibration was analyzed, showing that over 40 points the improvement in the IRB-140 robot accuracy is insignificant. With the minimum calibrated model and 30 measurement points, the deviation in TCP for each measurement point was also investigated, allowing a maximum error of 0.74 mm to be detected, which is lower than the error allowed by the automotive industry

in terms of parts manufactured by off-line programmed manipulators. Finally, a precision analysis of the minimum calibrated model was performed, in which position errors were reduced from 1.0 mm (in the first iteration) to 0.4 mm (in the last iteration)

## 7. ACKNOWLEDGMENTS

The authors are grateful to the University of Brasilia and to CAPES Foundation and the staff of the Robotics and Computer Vision Laboratory, who provided support for this research.

## 8. REFERENCES

- Agheli, M. and Nategh, M., 2009. "Identifying the kinematic parameters of hexapod machine tool". *World Academy of Science, Engineering and Technology*, Vol. 52, pp. 380–385.
- Bai, S. and Teo, M.Y., 2003. "Kinematic calibration and pose measurement of a medical parallel manipulator by optical position sensors". *Journal of Robotic Systems*, Vol. 20, No. 4, pp. 201–209.
- Bernard, R. and Albright, S., 1993. *Robot calibration*. Springer Science & Business Media.
- Duelen, G. and Schröer, K., 1991. "Robot calibration—method and results". *Robotics and Computer-Integrated Manufacturing*, Vol. 8, No. 4, pp. 223–231.
- Gao, G., Sun, G., Na, J., Guo, Y. and Wu, X., 2018. "Structural parameter identification for 6 dof industrial robots". *Mechanical Systems and Signal Processing*, Vol. 113, pp. 145–155.
- Ginani, L.S. and Motta, J.M.S., 2011. "Theoretical and practical aspects of robot calibration with experimental verification". *Journal of the Brazilian Society of Mechanical Sciences and Engineering*, Vol. 33, No. 1, pp. 15–21.
- Ha, I.C., 2008. "Kinematic parameter calibration method for industrial robot manipulator using the relative position". *Journal of mechanical science and technology*, Vol. 22, No. 6, p. 1084.
- Jang, J.H., Kim, S.H. and Kwak, Y.K., 2001. "Calibration of geometric and non-geometric errors of an industrial robot". *Robotica*, Vol. 19, No. 3, pp. 311–321.
- Liu, Y., Wu, J., Wang, L. and Wang, J., 2016. "Parameter identification algorithm of kinematic calibration in parallel manipulators". *Advances in Mechanical Engineering*, Vol. 8, No. 9, p. 1687814016667908.
- Motta, J., 1999. "Optimised robot calibration using a vision-based measurement system with a single camera".
- Motta, J.M.S.T.d., 2005. "An investigation of singularities in robot kinematic chains aiming at building robot calibration models for off-line programming". *Journal of the Brazilian Society of Mechanical Sciences and Engineering*, Vol. 27, No. 2, pp. 200–204.
- Motta, J.M.S., 2006. "Robot calibration: Modeling measurement and applications". In *Industrial Robotics: Programming, Simulation and Applications*, IntechOpen.
- Motta, J.M.S., De Carvalho, G.C. and McMaster, R., 2001. "Robot calibration using a 3d vision-based measurement system with a single camera". *Robotics and Computer-Integrated Manufacturing*, Vol. 17, No. 6, pp. 487–497.
- Motta, J.M.S., Llanos-Quintero, C.H. and Coral Sampaio, R., 2016. "Inverse kinematics and model calibration optimization of a five-dof robot for repairing the surface profiles of hydraulic turbine blades". *International Journal of Advanced Robotic Systems*, Vol. 13, No. 3, p. 114.
- Motta, J.M.S. and McMaster, R.S., 1999. "Modeling, optimizing and simulating robot calibration with accuracy improvement". *Journal of the Brazilian Society of Mechanical Sciences*, Vol. 21, No. 3, pp. 384–401.
- Santolaria, J., Aguilar, J.J., Yagüe, J.A. and Pastor, J., 2008. "Kinematic parameter estimation technique for calibration and repeatability improvement of articulated arm coordinate measuring machines". *Precision Engineering*, Vol. 32, No. 4, pp. 251–268.
- Schröer, K., Albright, S.L. and Grethlein, M., 1997. "Complete, minimal and model-continuous kinematic models for robot calibration". *Robotics and Computer-Integrated Manufacturing*, Vol. 13, No. 1, pp. 73–85.
- Wampler, C.W., Morgan, A. and Sommese, A., 1990. "Numerical continuation methods for solving polynomial systems arising in kinematics". *Journal of mechanical design*, Vol. 112, No. 1, pp. 59–68.
- Yang, X., Wu, L., Li, J. and Chen, K., 2014. "A minimal kinematic model for serial robot calibration using poe formula". *Robotics and Computer-Integrated Manufacturing*, Vol. 30, No. 3, pp. 326–334.
- Zhuang, H. and Roth, Z.S., 1996. *Camera-aided robot calibration*. CRC press.

## 9. RESPONSIBILITY NOTICE

The authors are the only responsible for the printed material included in this paper.